Radiation Patterns on a Budget: IEEE AP-S Student Design Challenge 2011

Andrew Temme, Donald VanderLaan, and Stephen Zajac

Department of Electrical and Computer Engineering
Michigan State University, East Lansing, MI, 48824 USA
E-mail: temmeand@msu.edu

Abstract

An important characteristic of an antenna is the radiation pattern, which determines in which direction(s) radiation is concentrated. Typical antenna radiation-pattern-measurement systems consist of measurement equipment and a controlled environment. Both of these elements can individually be prohibitively expensive, in terms of both cost and laboratory space. This paper outlines a low-cost (less than $1500) system for use at 2.4 GHz that is portable and requires a limited amount of space. Measurements are accomplished using a self-contained RF system, a simply constructed antenna rotator, a readily available data-acquisition and motor-controller circuit, and *MATLAB*. A key feature of this system is an extremely low-cost and simple rotary joint, which eliminates cable twisting.

Keywords: Antenna measurements; antenna radiation patterns; IEEE Antennas and Propagation Society; student activities; student experiments; computerized instrumentation; gain measurement; measurement techniques; IEEE AP-S Student Design Contest

1. Introduction

The radiation pattern of an antenna determines in what directions radiation from the antenna is concentrated. This allows for a signal to be sent or received in one particular direction or in multiple directions. When receiving a signal, the radiation pattern can help to reduce noise and increase the signal-to-noise ratio (SNR). While simulations provide relatively good predictions of antenna patterns, differences from simulations can be substantial, due to construction techniques and factors not included in simulations.

Typical antenna-pattern-measurement ranges vary in cost, from thousands of to hundreds of thousands of dollars. Measurement equipment alone can be more than ten thousand dollars, not to mention construction materials, manufacturing, and installation. This high cost can be prohibitive for schools and small businesses. For these users, extreme accuracy may not be needed. For such a case, the design may be simplified and the cost significantly reduced.

The objective of this project was to design an antenna radiation-pattern measurement system with ±0.5 dB accuracy if placed in an anechoic environment, on a budget of $1500.

2. Goals and Specifications

As given in the Design Challenge announcement, the goals and specifications were the following:

- Design a measurement system that can be used to find the gain and radiation pattern of a test antenna. An anechoic chamber is not required, so inaccuracies due to reflections by nearby objects are inevitable. However, a reasonable argument must be presented that the gain measurement accuracy would be ±0.5 dB in an anechoic environment.
- The system must be safe and durable, easily reproducible by others, inexpensive, and portable so that it can be demonstrated at the Symposium.
- The system must operate at 2.4 GHz, generate its own signal, have its own power supply, and fit on a table or two closely spaced tables. Readily available software (e.g., student versions of *C*, *MATLAB*, *Visual Basic*, *LabView*) or free software packages may be used.

- The total cost for reproduction of the system must be less than $1500. All equipment and software (except for a computer, if needed) must be included in the budget. The use of a computer is allowed and does not have to be included in the $1500 budget [1].

3. System Overview

To determine the radiation pattern of an antenna, herein referred to as the antenna under test (AUT), one needs an RF energy source, a reference antenna, a mechanism for rotating either the reference antenna or the AUT, and an RF power detector. One antenna is kept stationary, while the second antenna is rotated relative to the other antenna. The RF signal is transmitted from one antenna and received by the other antenna. The received signal is measured and recorded in relation to the angle between a reference point and the AUT.

The system outlined in this paper keeps the reference antenna stationary and uses it as the transmitting antenna, while the AUT is rotated while receiving the transmitted signal.

The assembled system is shown in operation in Figure 1.

3.1 Theory of Operation

Power was supplied to the system from a standard 120 V ac wall outlet, which was converted to 5, 12, and 36 V dc. The 5 V dc supply was used to power the RF source, amplifiers, and detector along with other low-power electronics. The 12 V dc supply was used to power the control logic of the data-acquisition and motor-controller circuit, while the 36 V dc was used to power the motor.

Figure 1. The assembled system.

The 5 V and 12 V power supplies were implemented using IC linear regulators, as opposed to switching regulators. This choice was made to avoid the interference that switching regulators can generate. This interference at the fundamental switching frequency can be quite significant, with harmonics extending well into the frequency range of the selected power detector. The 36 V power supply was implemented using a discrete MOSFET as a linear regulator. This produced a higher output-current limit than IC regulators could provide, allowing the system to drive more-demanding motor loads.

The 120 V ac was first transformed down to a lower ac voltage using a toroidal transformer. The secondary voltage of these transformers was picked to allow for a 2 V drop across the diode bridge, and a 2 V to 7 V drop across the liner regulator, ensuring that the power supply stayed in regulation at all times. This voltage was then full-wave rectified by a diode bridge, and smoothed by a filter capacitor. The resulting dc voltage was finally regulated down to the appropriate voltage by the linear regulator in each power supply.

Printed-circuit boards for all three power supplies were provided by [2], and customized to fit the specific voltage requirements of the project.

The RF signal was generated using a voltage-controlled oscillator (VCO), operating between 2.315 and 2.536 GHz. The signal was amplified to approximately 16 dBm before being transmitted from the reference antenna.

The reference antenna was a stationary, reflector-type antenna, purchased from [3]. This antenna was selected for its relatively high gain (15 dBi) and narrow beamwidth (16° horizontal, 21° vertical) [3]. This helped to focus the transmitted power on the AUT, while helping to reduce reflections from surrounding areas.

Given the above reference antenna and assuming a separation between the two antennas of one meter, the path loss was calculated to be 40.05 dB, using the Friis equation [4]. The received signal was amplified by 14 dB, passed to a bandpass filter, and then to a logarithmic-law power detector. The detector had a dynamic range of −60 dBm to 0 dBm. The typical insertion loss of the filter was 1.8 dB at the operating frequency. Given the above values, the gain of the AUT could theoretically have a maximum value of −1.5 dBi, while nulls could be measured down to −60 dBi. If the amplifier on the receiver end were to be removed, these values would change to −47.5 and 12.5 dBi.

The AUT was mounted on a Styrofoam antenna stand, which sat on top of a small, rotating table. A power measurement was taken at a user-specified number of angles as the AUT was rotated a full 360°.

Rotation was achieved using a low-cost stepper motor and motor controller, which was controlled by the computer over an RS-232 connection. The cost and feature set were considered when choosing a controller, and the selected model provided up to four digital inputs/outputs (selectable) and two eight-bit

analog inputs. However, only four inputs/outputs could be used simultaneously, which was sufficient for our application.

The rotating table was supported using a hollow, low-cost circular ball-bearing "lazy-Susan" turntable. The motor controller operated a motor that was connected to a hollow shaft on the rotary table by a rubber belt. This hollow shaft was mounted through the lazy-Susan bearing. The mechanical gear ratio was found to be 2.7397 by counting the number of steps needed to rotate the table 10 continuous revolutions. Combined with 360 half-steps, the angular resolution of the mechanical rotator was 0.365°; alternately put, the rotator could point the antenna in 986 unique directions.

The power detector output a dc signal between 0.5 and 2.2 V. This output signal, ground connection, and the power for the detector were carried through the rotator table using a 6.35 mm TRS plug and jack, which served as a rotary-joint connector as shown in Figure 2. This rotary joint eliminated twisting of the cables, which is typically a major problem. Commercial rotary joints are expensive, whereas the rotary joint used here cost less than ten dollars.

The TRS plug was mounted inside the hollow shaft fixed to the rotation plate. This was done such that the TRS plug, hollow drive shaft, and lazy-Susan bearing were all concentric and rotated about the same axis, which itself was at the center of the rotation plate. Once through the rotator table, the dc signal was amplified to 0 and 5 V – to utilize all eight ADC bits – and carried to the analog-to-digital converter on the motor-controller board. There, it was read and transmitted to the computer over an RS-232 link.

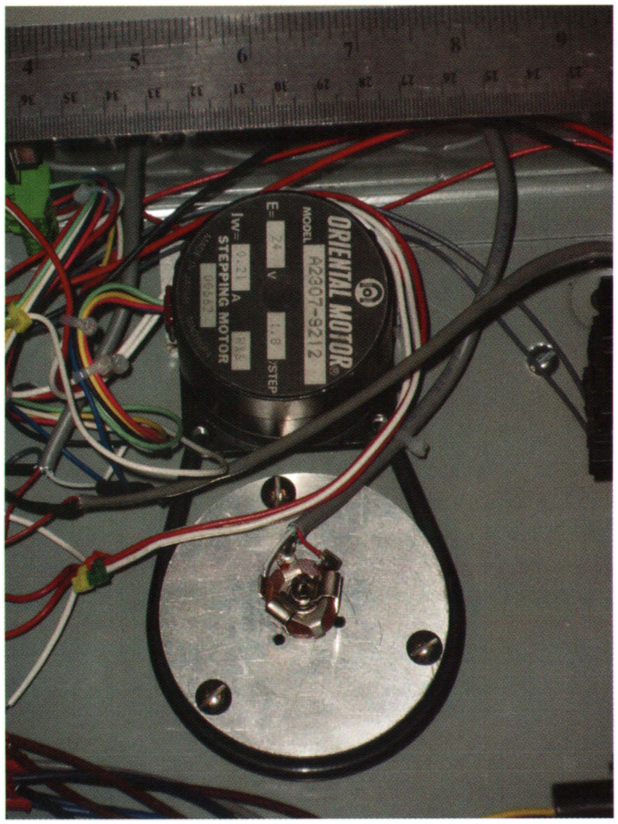

Figure 2. The rotary joint, which eliminates twisting in the cables.

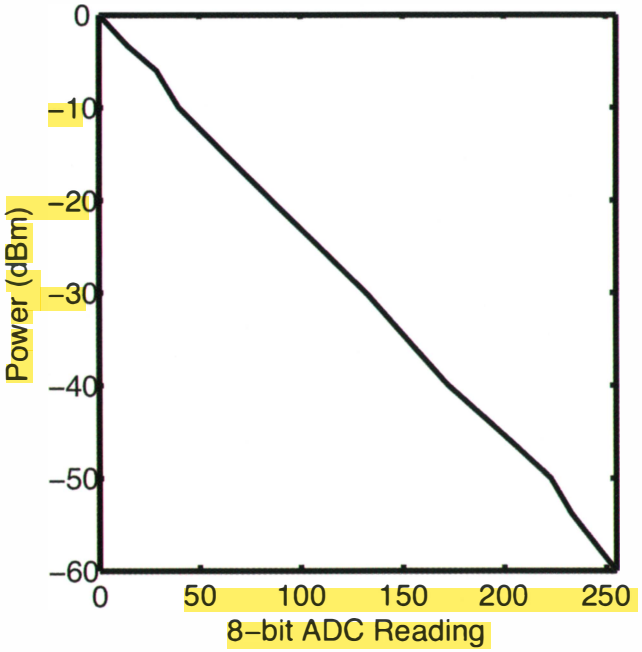

Figure 3. The calibration data for the power detector.

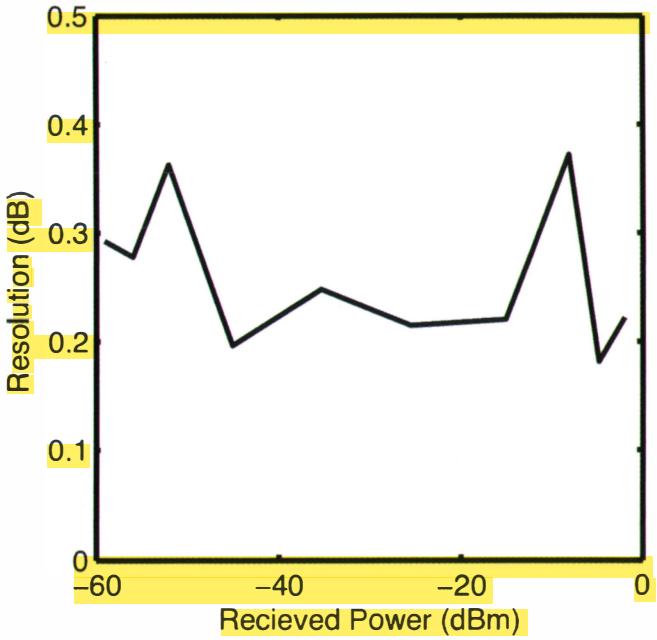

Figure 4. The detector resolution as a function of the input power.

3.2 System Accuracy

An ideal anechoic environment has two defining features that would make an antenna-pattern measurement system more accurate. First, all six sides of the room are lined with RF absorber material to prevent multiple reflections that would affect the accuracy of the system. Second, the entire room is shielded from external radiation that could also affect system accuracy. With a budget of $1500 and a requirement that the system be portable, these two criteria had to be met through alternative means.

To reduce multiple reflections, a two-fold approach was used. First, the reference antenna was selected to have a very narrow beamwidth, such that at a distance of six feet, the main beam had a diameter of less than two feet. Second, a single RF absorber was placed behind the AUT and inline with the reference antenna. The industry-standard size of RF absorber material is a two foot by two foot square, which in this setup would absorb most of the radiated power from the transmitted antenna, which would otherwise be reflected.

The choice of RF absorber material came down to two factors: size and absorption performance in dB at a given frequency. In general, the absorption is directly proportional to the height of the material. For example, an absorber with a height of 72 in will outperform a three-inch high absorber in terms of attenuation. The 72 in high absorber also maintains this absorption at frequencies lower than the three-inch model. In this application, at 2.4 GHz, the ideal height was approximately eight inches for a pyramidal absorber. The specific model selected had a one-way absorption of −35 dB. The only concern then became reflections of the sidelobes of the reference antenna, which were very small, due to the choice of a narrow-beamwidth antenna.

The second criteria of an anechoic environment is the reduction of interference from external signals. With modern spectrum analyzers, the resolution bandwidth can go as low at 1 Hz, making it very easy to distinguish between the test signal and interference. Due to budget requirements, this project used a diode detector with a bandwidth of 8 GHz. With this bandwidth, it was impossible to distinguish between the power received by the AUT and noise at other frequencies. A bandpass filter was placed in front of the power detector to isolate the AUT's signal. The Mini-Circuits bandpass filter used had a −3 dB bandwidth of 220 MHz.

The detector was characterized over the input-power range for power received as a function of voltage read. The results are shown in Figure 3. Using these data, the resolution of the system was derived, and is given in Figure 4. Gain measurements could be resolved to better than ±0.5 dB over the entire detected power range.

A calibration procedure involving three different measurements was used to make absolute gain measurements. First, the transmitter was connected directly to the receiver, and a measurement was taken. Next, a known attenuator was placed between the transmitter and the receiver. These two measurements were used to identify system losses. Finally, a measurement was taken using two identical antennas, and the Friis equation was used to determine the gain of the reference antenna.

4. Schematics, Parts, and Budget

4.1 System Schematics

Figure 5 shows a block diagram of the system. Schematics for the power supplies can be found online at [2]. Motor-controller documentation is available from [5]. Datasheets for the RF components are available from [6]. Assembly instructions for the reference antenna are available from [3].

4.2 List of Parts and Budget

Table 1 gives a list of the parts and the associated cost. The total cost to replicate the system was $1,084.45.

5. Assembly Instructions

5.1 Rotator Top and Cable Rotator

In the top of the rotator base, use a hole saw to cut a hole that is slightly larger than the hollow shaft. Also, drill holes for mounting the lazy-Susan bearing and all other components.

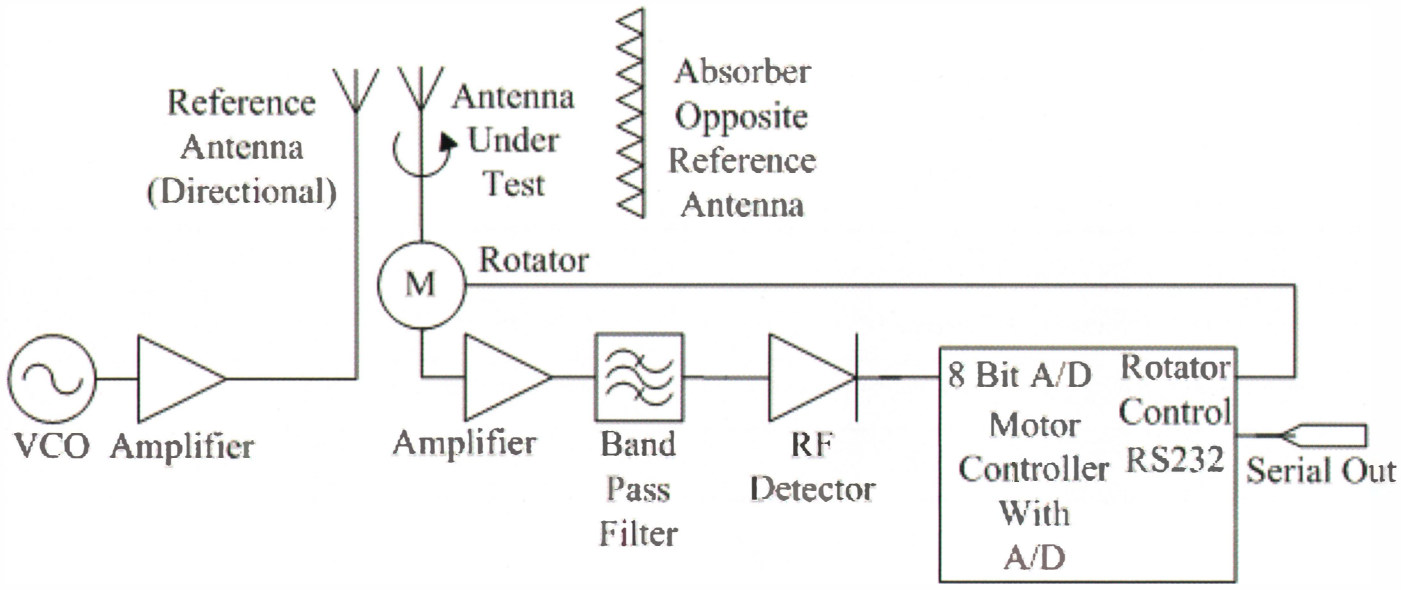

Figure 5. A block diagram of the system.

Table 1. The budget and parts list.

Qty	Item	Description	Supplier	Part Number	Unit Price ($)	Total ($)
1	Lazy Susan	Lazy Susan bearing, 6 in	Ace Hardware	9548	6.50	6.50
2	Components	1.5 in extruded TO-220 heatsink	AMB Audio Shop	529802B00000	2.00	4.00
1	Components	International Rectifier power MOSFET	AMB Audio Shop	IRLZ24N	3.50	3.50
1	Power Supply	Power Supply Circuit Boards	AMB Audio Shop	Sigma 11	10.00	10.00
2	Circuit Boards	Power Supply Circuit Boards	AMB Audio Shop	Sigma 25	7.00	14.00
1	Motor	Stepper Motor	Anaheim Automation	17L9	97.00	97.00
1	Transformer	15VA, 12V + 12V	Avel Lindberg	Y236002	20.23	20.23
1	Transformer	15VA, 9V + 9V	Avel Lindberg	Y236001	20.23	20.23
1	Transformer	50VA, 18V + 18V	Avel Lindberg	Y236204	25.51	25.51
1	Absorber	2 ft × 2 ft absorber	ETS-Lindgren	EHP-8PCL	60.00	60.00
1	Mounting Hardware	Mounting Hardware	Hardware store		20.00	20.00
2	Reflector Antenna	2.4 GHz 15 dBi Die-cast Grid Antenna	L-Com	HG2415G-NF	36.62	73.24
1	Cinder Block	Cinder block	Lowes		1.00	1.00
1	Clamp	Clamp	Lowes		5.00	5.00
1	PVC Pipe	PVC pipe, Schedule 40, 1 1/4 in, 6 ft	Lowes		2.33	2.33
2	Antenna Stand	Rose Covers used as antennas stands	Lowes		6.23	12.46
1	*MATLAB*	*MATLAB* Student Version	MathWorks		100.00	100.00
1	Rotator Base	Indoor Steel Enclosure, 10 in by 10 in by 6 in	McMaster-Carr	75065K38	27.79	27.79
1	VCO	2.4 GHz - 2.67 GHz Oscillator	Mini-Circuits	ZX95-2536C-S+	44.95	44.95
1	Attenuator	3 dB Attenuator	Mini-Circuits	VAT-3+	11.95	11.95
1	Filter	Bandpass filter	Mini-Circuits	VBF-2360+	34.95	34.95
2	Amplifier	Power Amplifier	Mini-Circuits	ZX60-272LN-S+	39.95	79.90
1	Detector	Power Detector	Mini-Circuits	ZX47-60-S+	89.95	89.95
1	Components	Misc. Components: potentiometers, heat shrink, terminal blocks, etc. as per personal manufacturing preference	Mouser		30.00	30.00
1	Adapter	N-Male to SMA Female adapter	Mouser	523-242113	7.50	7.50
1	Cable	SMA Male RG142, 36 in	Mouser	523-135101-07-36.00	25.49	25.49
1	Adapter	SMA-Female to SMA-Female adapter	Mouser	523-132169	3.97	3.97
1	Adapter	SMA-Male to SMA-Male adapter	Mouser	523-132168	5.16	5.16
1	Components	Power Supply Components	Mouser/ AMB Audio		66.84	66.84
1	Hollow Pipe	Schedule 80 Al Bare Pipe 6061 T6 - 10 in	OnlineMetals.com		22.00	22.00
1	Motor Controller	Stepper Motor Controller	Pontech	STP100	159.00	159.00
					Total	**$1,084.45**

Attach the plastic rotator table top to the lazy-Susan bearing, and then the lazy-Susan bearing to the rotator base. Install the 6.35 mm TRS plug through the hollow shaft. Figure 6 shows the rotator table top.

Mount the motor controller, motor, power socket, and any other desired accessories on the inside of the rotator base. Figure 7 shows one possible assembly configuration.

5.2 Power Supplies

Assemble the power-supply kits according to the supplier's instructions. Mount the power-supply circuit boards and associated transformers inside the rotator base. Figure 8 shows the power supplies and transformers.

5.3 RF Source

Connect the VCO (ZX95-2536C+) to the 3 dB attenuator (VAT-3+). Connect the amplifier (ZX60-272LN+) to the other end of the attenuator using an SMA male-to-male barrel adapter (SM-SM50+): see Figure 9. Tighten the connections to 5 in-lbs.

5.4 RF Receiver

The receiver consisted of an amplifier, filter, and power detector. Connect the filter (VBF-2360+) between the amplifier (ZX60-272LN+) and the RF detector (ZX47-60-S+). Tighten connections to 5 in-lbs. Attach the detector to the top of the rotator table, and connect the power, ground, and signal cables from the rotary-joint cable to the detector.

5.4 Reference Antenna

Assemble the two reference reflector antennas according to the supplier's instructions [3]. Using the supplied mounting hardware, mount one reference antenna to the top of the PVC pipe according to the supplier's instructions. Use a C-clamp to attach the pipe to the cinder block, or create any other stand for the antenna. Run a dc power cable to the reference antenna from the rotator base. Connect the dc power cable to the RF source components assembled earlier. Using an N-to-SMA adapter, connect the RF source to the reference antenna. Use a potentiometer to adjust V_{tune} .

5.5 Antenna Stand

Glue the bases of the two rose covers together to form a stand for the test antenna, using Elmer's glue. Remove just enough Styrofoam from the bottom of the stand (the top of one of the rose covers) for the detector and cables so that the stand

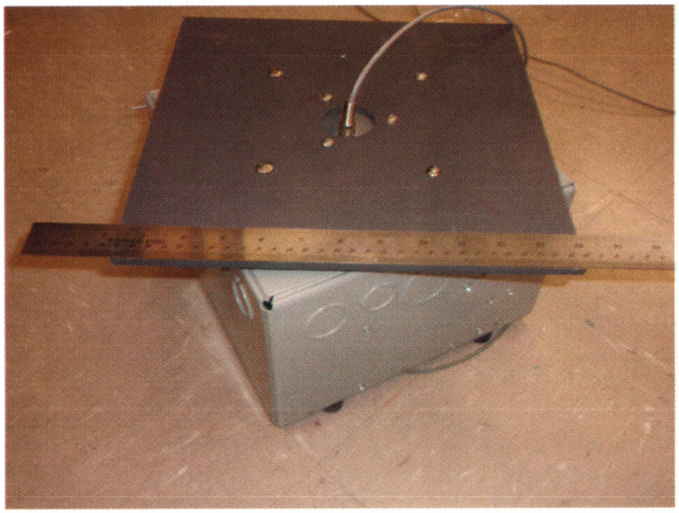

Figure 6. The rotator table top.

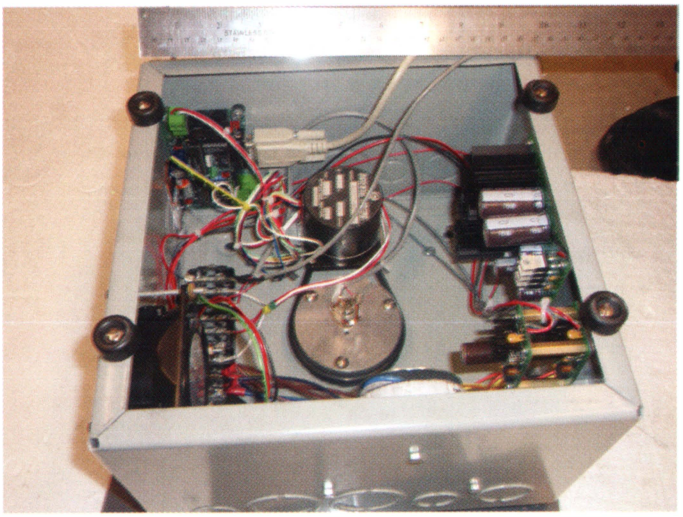

Figure 7. The rotator base.

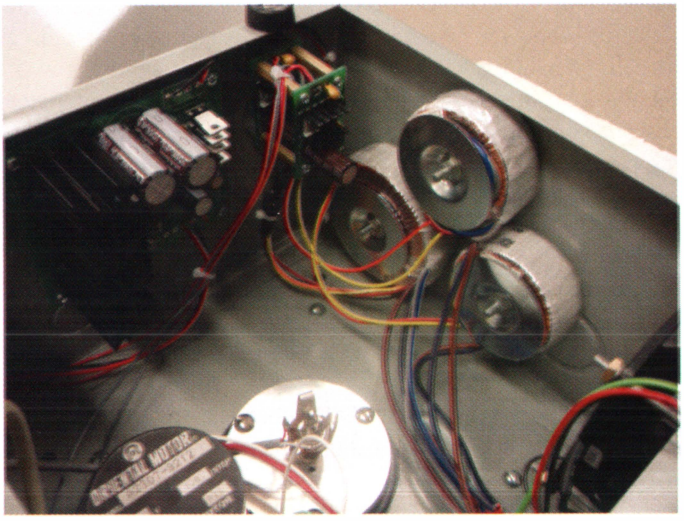

Figure 8. The transformers (right), power supplies (left), and rotary joint (bottom).

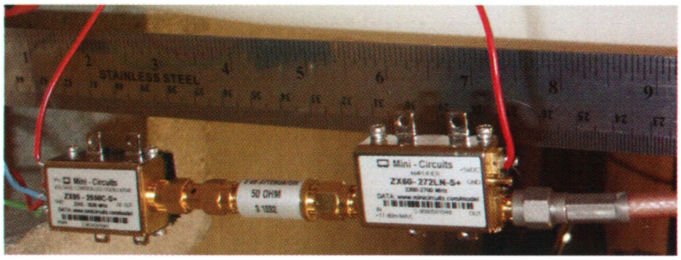

Figure 9. The VCO (left), 3 dB attenuator (center), and 14 dB linear amplifier (right).

sits flush on top of the rotator table. Place a small hole in the top of the stand, and feed an SMA cable through the hole and connect it to the RF detector. Position the stand on the rotator table top, and affix using Velcro or other suitable method that will keep the stand upright when a test antenna is placed atop of it. The unconnected end of the SMA cable is the antenna-under-test port (AUT port).

6. Operating Instructions

Always use a grounding wrist strap or other grounding device when touching any metal parts of the system, including cable connectors or antennas.

The antenna-pattern measurement system emits RF energy whenever power is turned on at the base of the rotator. Turn off power whenever making any connections, or when working in front of the reference antenna.

6.1 Calibration

The system was calibrated using three measurements. First, measure the received power when the transmitter is connected directly to the receiver. Next, place a known attenuator between the transmitter and receiver, and measure the received power. These two measurements, along with knowing the transmitted power and the value of the attenuator, are used to calibrate the ADC reading to the correct received power. Finally, a third measurement is taken when both reference antennas are connected to the system, positioned with matching polarizations and pointed with the maximum gain for each antenna at the other one. The Friis equation is then used to find the absolute gain of the reference antenna.

6.2 Measurement Preparation

The antenna under test (AUT) should be placed on top of the Styrofoam antenna stand. Align the reference antenna to be coplanar with the desired measurement plane of the AUT. Align the polarizations of the AUT and reference antenna. Ensure that the AUT is secured and will not move during multiple, complete revolutions.

6.3 Software

A graphical user interface was created to handle the calibration procedure and measurement procedure. The user is able to specify measurement parameters such as the number of points measured and the speed of the motor. The measured value is sampled for each angle, corrected using the calibration values, and displayed on a polar plot.

7. Example Results

Using the system outlined above, the radiation pattern of a tuned dipole antenna was measured, and this is plotted in Figure 10. One could see the expected figure-eight pattern of a dipole antenna. The pattern also showed the maximum gain of the dipole to be between approximately –2 and –3 dBi. Other measured antennas included monopoles, Wi-Fi "cantannas," and antennas from [7].

8. Future Work

8.1 Power Detector

A microstrip-based power detector was prototyped for the system, and is shown in Figure 11. The selected power detector was an Analog Devices logarithmic detector AD8313 [8].

The connection to the circuit board was made using an SMA jack. The circuit-board design was derived from the suggested design given in the datasheet found online at [8]. Fabrication of the circuit board was done in-house using a photo-etching process. The circuit was constructed on 31 mil thick Rogers Duroid 5880 circuit board, which was sent as a sample from Rogers.

Initial testing showed inconsistent results in measured power. Resistors and matching networks were varied in order to adjust the slope of the output and the transferred power. A coaxial power detector from Mini-Circuits was substituted into the current design while work continues on the microstrip-based power detector.

8.2 Microstrip Filters

A filter was needed for the microstrip-based power detector presented in the previous section. A design procedure for side-coupled bandpass filters was presented by Pozar in [9]. Lumped-element filters are normally designed using low-pass-filter prototype values, which are then frequency and impedance scaled to meet a specific filter application. Pozar's method used the same low-pass-filter prototype values, but implemented resistor and capacitor values with edge-coupled microstrip lines instead of lumped elements.

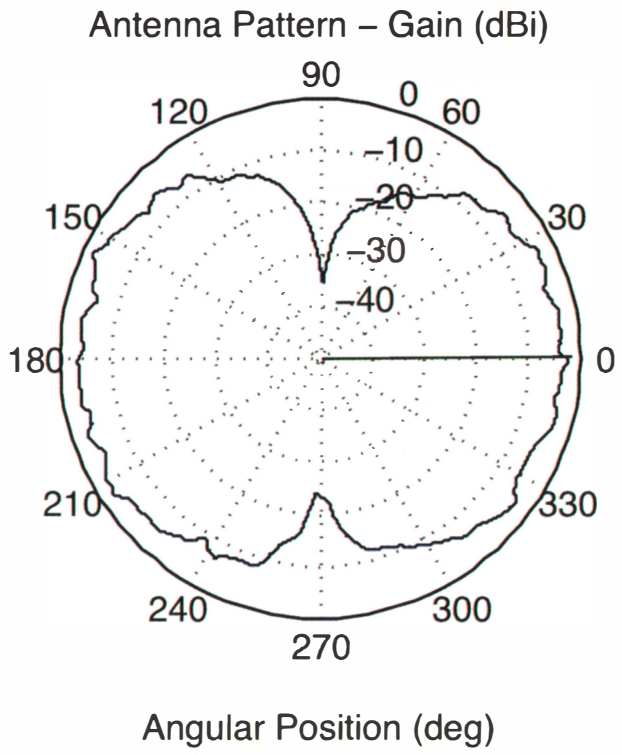

Figure 10. The pattern for a dipole antenna.

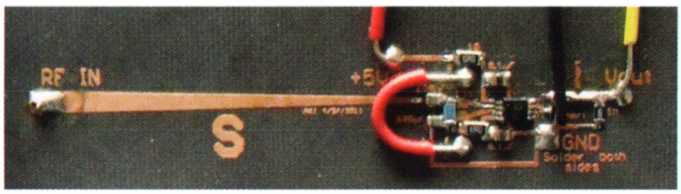

Figure 11. A microstrip-based power detector.

This first step was to pick the order and desired response of the filter. An Nth order filter is implemented using $N+1$ edge-coupled microstrip lines, where the roll-off between the pass band and stop band is $N \times 20$ dB/dec. A choice of $N = 3$ provided a good compromise between filter size and attenuation performance. The filter's response is specified in terms of pass-band ripple and stop-band attenuation. For example, Butterworth-type filters have a flat pass-band, while Chebyshev-type filters have higher stop-band attenuation, at the expense of pass-band ripple. For this project, stop-band attenuation was more important that a flat pass-band, so 3 dB equal-ripple low-pass-filter prototype constants were selected.

The next step was to set the fractional bandwidth of the filter, which is defined as BW/FO. This fractional bandwidth, along with the low-pass prototype constants, were then used to calculate the admittance inverter constants for each edge-coupled microstrip section. Finally, the admittance inverter constants could be used to determine the required even- and odd-mode impedances of each microstrip section.

Given a specific circuit-board material and thickness, the width (W) of each microstrip, and the spacing (S) between adjacent microstrip lines, can be numerically determined to implement the required even- and odd-mode impedances. The length (L) of each edge-coupled microstrip section determines the center frequency of the filter, and should be a quarter wavelength. With this length picked to give a center frequency of 2.4 GHz, the filter design was complete.

Ansoft *HFSS* [10] was used to verify the design shown in Figure 12. The dimensions of the completed filter were 3.75 in × 2 in, which was small enough to be placed on the antenna-rotator platform. The simulated attenuation performance, S_{21}, is shown in Figure 13. The -3 dB bandwidth was about 150 MHz, and the insertion loss at 2.4 GHz was 2.2 dB. To decrease the bandwidth, the odd-mode impedance could be increased, which effectively increased the spacing (S) between adjacent microstrip lines. This also increased the insertion loss, since the coupling between microstrip lines was reduced, so there was a minimum practical bandwidth that could be obtained. An insertion loss of 2 dB was determined to be a reasonable compromise for reduced bandwidth.

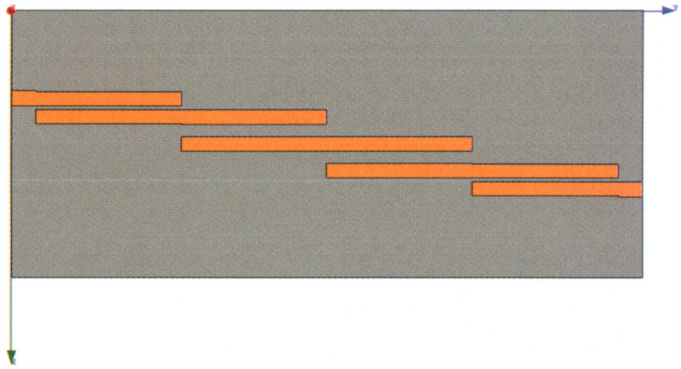

Figure 12. The filter design.

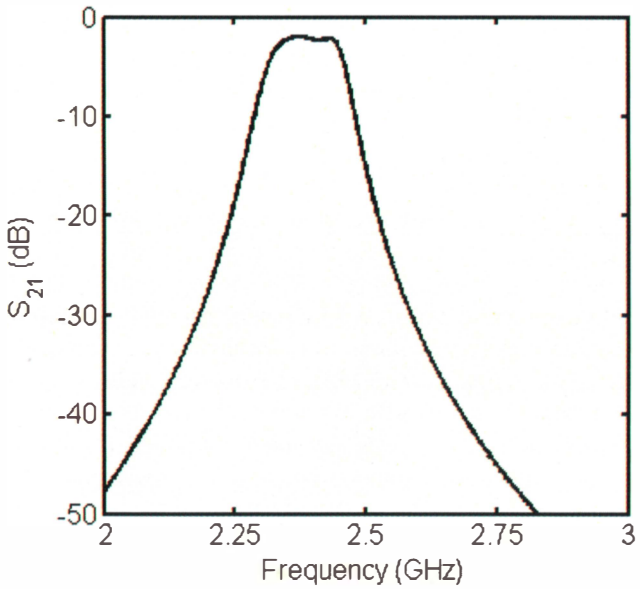

Figure 13. The response of the described filter design.

9. Conclusion

The system described herein was a low-cost implementation of an antenna-pattern acquisition system for characterization at 2.4 GHz. The system satisfied all the announcement requirements: accuracy to within ±0.5 dB for anechoic operation, durable, portable, reproducible, self-contained and stand-alone, and it could be implemented for under $1500, not including the price of a computer.

In addition to the aforementioned requirements, a number of other features and innovations were added to further the utility of the system. First, antenna rotation systems often deal with cord-tangling problems as the cord wraps around the antenna stand. Not only does this require the antenna to reverse rotation and unwrap the cord after pattern acquisition, but it also presents the possibility that the cord may catch on an anechoic spike and tip the entire antenna and stand over: landing on and damaging the anechoic floor. Systems that bypass this requirement often employ an RF rotary joint, which has finite life and – of significant concern here – can be very costly. Instead of transferring the RF signal across the plane of rotation, this implementation moved the detector across the rotation plane such that it was fixed with respect to the rotating antenna-under-test coordinate system. Therefore, the rotary joint had to only pass very-low-frequency signals. A $5.00 TRS plug and socket (intended for audio applications) was more then sufficient. Although not intended for extended rotation, it could be easily and cheaply replaced should the need arise.

Another innovation, concerning the reduction of pattern-acquisition time and the increase of angular sampling, was the application of the "equivalent time sampling" modes often seen in oscilloscope technology. As rotation was achieved using a stepper motor, either the motor had to be stopped at each angle for measurement, or it had to be rotated continuously and slowly enough to acquire the gain at the desired number of angular samples. The latter required the system to be able to index the current position, such as to compensate for acceleration and a non-ideal motion profile, which was implemented in our system. However, continuous rotation at low velocities is prone to resonance and requires a controller either with micro-stepping or electronic viscosity, features that are found only on more cost-prohibitive controllers. To alleviate this problem, the antenna was instead rotated at a rate above resonance, and an "equivalent sampling" methodology was used. The antenna makes multiple revolutions, each filling in samples between those taken in prior rotations: just as an "equivalent time sampling" oscilloscope requires multiple periods in order to obtain a sufficiently sampled waveform. For oscilloscope applications, this meant the technique was restricted to repetitive waveforms. However, here this was not a restriction: a complete rotation of the antenna presented the system exactly as it was any integer number of rotations in the past. Therefore, this system was able to acquire very high angular sampling while still keeping the acquisition time to a minimum. The acquisition time greatly depended on the accuracy desired, but ranged from under 10 seconds for crude estimates to anything on up.

The system was experimentally found to have a dynamic range of 60 dB, more then adequate for most antenna characterization. The system was set up to measure patterns falling into either −61.6 to −1.5 dBi or −47.5 to 12.5 dBi. However, additional amplifiers or attenuators could be inserted to achieve most practical ranges with less than 60 dB of dynamic range.

10. Acknowledgment

The authors would like to thank Dr. Edward Rothwell for his guidance on this project, and Raoul Ouedraogo for his help in the manufacturing of the needed circuit boards.

This material is partially based upon works supported by the National Science Foundation Graduate Research Fellowship under Grant No. DGE0802267.

11. References

1. IEEE Antennas and Propagation Society, "IEEE AP-S Student Design Challenge 2011: Radiation Patterns on a Budget," available at http://www.apsursi2011.org/StudentDesignChallenge.asp.

2. AMB Audio Laboratories, "The sigma11 Regulated Power Supply," available at http://www.amb.org/audio/sigma11/.

3. L-com Global Connectivity, "2.4 GHz 15 dBi Die-Cast Grid Antenna – 12 in N-Female Connector – HG2415G-NF," available at http://www.l-com.com/item.aspx?id=21694.

4. D. Archer, "LearningMeasure.com – Friis Transmission Equation Calculator," available at http:// www.learningmeasure.com/cgi-bin/calculators/friis.pl.

5. Pontech, "STP100 – PONTECH," available at http:// www.pontech.com/details/120.

6. Mini-Circuits, "Mini-Circuits RF/IF Designer's Guide," available at http://www.minicircuits.com/.

7. R. Ouedraogo and E. Rothwell, "Metamaterial Inspired Patch Antenna Miniaturization Technique," IEEE International Symposium on Antennas and Propagation *Digest*, July 2010, pp. 1-4.

8. Analog Devices, "AD8313 | 0.1-2.5 GHz, 70 dB Logarithmic Detector/Controller | Detectors | RF/IF ICs | Analog Devices," available at http://www.analog.com/en/rfif-components/detectors/ad8313/products/product.html.

9. D. M. Pozar, *Microwave Engineering*, New York, Wiley, 1997.

10. Ansoft, "HFSS," available at http:// www.ansoft.com/products/hf/hfss/.

Introducing the Authors

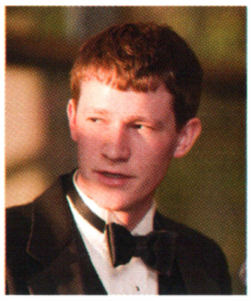

Andrew Temme earned his BS in Electrical Engineering from Michigan State University, East Lansing, MI, in May, 2010. As an undergraduate, he worked in the Smart Microsystems Laboratory, Michigan State University, before joining the Electromagnetics Research Group in 2008, where he remains. His interests include through-wall radar, search and rescue, combustion, antenna design, and microwave measurement techniques.

Don VanderLaan completed a BS in Electrical Engineering at Michigan State University in May 2009. Don is an NSF Graduate Research Fellowship recipient, and works with the Biomedical Ultrasonics & Electromagnetics laboratory at Michigan State University. His interests are thermal therapy/hyperthermia treatment achieved through focused ultrasound, as well as modeling wave propagation in tissue and similarly dispersive media. He is currently researching the theoretical constraints causality imposes on dispersion relations for Green's-function-based tissue modeling.

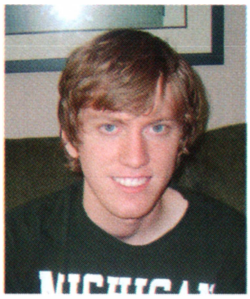

Stephen Zajac received his BS in Electrical Engineering from Michigan State University in 2009, and is currently working towards the MS degree in Electrical Engineering, also at Michigan State University. Stephen is a graduate teaching assistant in the engineering department, having taught lab courses ranging from circuits to optics. He is also a graduate research assistant at the National Superconducting Cyclotron Laboratory, working on high-power RF amplifier development. His interests include circuit design at audio and microwave frequencies, along with practical applications of EM theory.